

Are the Magnetic Fields Radial in the Solar Polar Region?

Xudong Sun (孙旭东)  ¹, Yang Liu (刘扬)  ², Ivan Milić  ^{3,4,5} and Ana Belén Griñón-Marín  ^{2,6,7}

¹*Institute for Astronomy, University of Hawai‘i at Mānoa, Pukalani, HI 96768, USA; xudongs@hawaii.edu*

²*W.W. Hansen Experimental Physics Laboratory, Stanford University, Stanford, CA 94305, USA*

³*Department of Physics, University of Colorado, Boulder, CO 80309, USA*

⁴*Laboratory for Atmospheric and Space Physics, University of Colorado, Boulder, CO 80303, USA*

⁵*National Solar Observatory, Boulder, CO 80303, USA*

⁶*Institute of Theoretical Astrophysics, University of Oslo, N-0315 Oslo, Norway*

⁷*Rosslund Centre for Solar Physics, University of Oslo, N-0315 Oslo, Norway*

(Received May 25, 2021; Accepted June 2, 2021)

ABSTRACT

We investigate the orientation of the photospheric magnetic fields in the solar polar region using observations from the Helioseismic and Magnetic Imager (HMI). Inside small patches of significant polarization, the inferred magnetic field vectors at $1''$ scale appear to systematically deviate from the radial direction. Most tilt towards the pole; all are more inclined toward the plane of sky compared to the radial vector. These results, however, depend on the “filling factor” f that characterizes the unresolved magnetic structures. The default, uninformative $f \equiv 1$ for HMI will incur larger inclination and less radial fields than $f < 1$. The observed trend may be a systematic bias inherent to the limited resolution.

Keywords: Solar magnetic fields (1503); Solar photosphere (1518)

The photospheric magnetic fields in the solar polar region (polar fields) are often assumed to be radial. The radial component B_r is then related to the line-of-sight (LOS) component B_l as $B_r = B_l \mu^{-1}$, where μ is the cosine of the heliocentric angle. Both observation and modeling lend support to the assumption for spatial scales greater than several heliographic degrees (Svalgaard et al. 1978; Wang & Sheeley 1992; Petrie & Patrikeeva 2009).

The polar fields are spatially non-uniform. Most polarization signals come from small, isolated patches a few megameter wide, covering at most a few percent of the polar region (Figure 1(a)). The intrinsic field strength B can exceed 1 kG based on the high-resolution observations ($0''.3$) from the *Hinode* satellite (Tsuneta et al. 2008).

We investigate the orientation of the magnetic field vectors \mathbf{B} inside these patches using the Helioseismic and Magnetic Imager (HMI) aboard the *Solar Dynamics Observatory*. HMI provides full-disk Stokes observations of the photospheric Fe I 617.3 nm line. The spatial resolution is $1''$ with a $0''.5$ pixel $^{-1}$ plate scale; the spectral sampling is performed at six wavelengths. We evaluate the polarization degree for each pixel in the southern polar region measured on March 4, 2015, and select about 1000 pixels (0.2% of total) whose signal is above 5σ for further analysis. The field of view is limited to $[-85^\circ, -60^\circ]$ latitude, and $[-75^\circ, 75^\circ]$ longitude. The HMI pipeline infers \mathbf{B} and the formal measurement uncertainties (Hoeksema et al. 2014).

The magnetic inclination γ , defined as 0° toward and 180° away from the observer, exhibits an interesting trend. The values of $|\cos \gamma|$ are invariably smaller than μ (Figure 1(b)). In other words, the \mathbf{B} vectors are more inclined toward the plane of sky compared to the local radial vector. About 93% of the pixels also have $\text{sgn}(B_r)B_\theta B^{-1} > 0$, where B_r and B_θ are the radial and meridional components in a heliocentric spherical coordinate. This means that most \mathbf{B} vectors tilt toward the pole. The median deviation from the radial direction is 18° .

Is this trend genuine, or is it due to some systematic bias? We explore the effect of the “filling factor” parameter f in the magnetic inference procedure, which represents the sub-pixel fractional area occupied by the unresolved magnetic structures. In the weak-field approximation (Jefferies & Mickey 1991), \mathbf{B} depends on the Stokes parameters (Q, U, V) as

$$\begin{aligned} fB \cos \gamma &\propto V, \\ fB^2 \sin^2 \gamma &\propto (Q^2 + U^2)^{1/2}. \end{aligned} \tag{1}$$

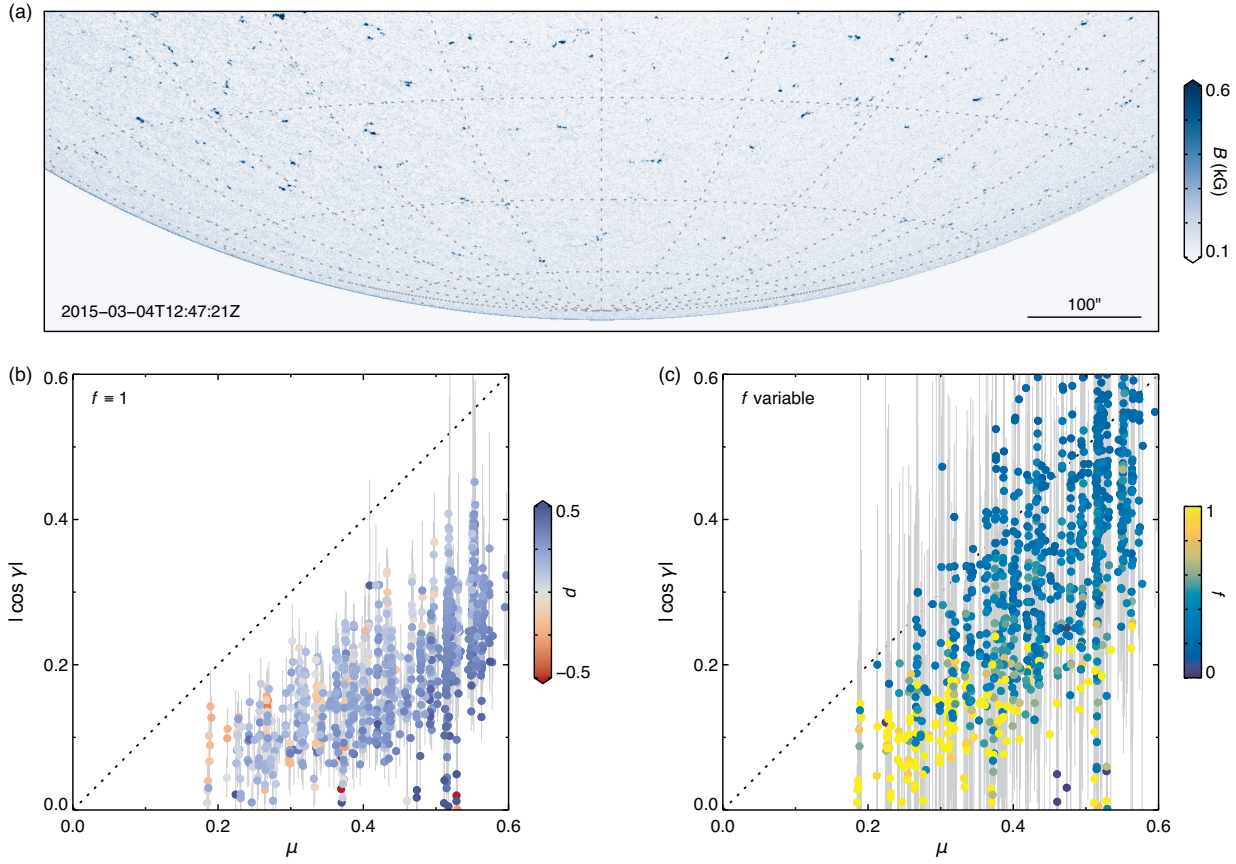


Figure 1. HMI observations of the southern polar region. (a) Map of B , inferred with $f \equiv 1$. The dotted lines show the latitude (longitude) with 10° (15°) spacing. (b) Scatter plot of μ vs $|\cos \gamma|$, inferred with $f \equiv 1$. The colors indicate $p = \text{sgn}(B_r)B_\theta B^{-1}$. For the southern hemisphere, \mathbf{B} tilts toward the pole if $p > 0$. The error bars show $\pm \sigma_\gamma \sin \gamma$, where σ_γ is the formal uncertainty of γ . (c) Same as (b), but inferred with f as a free parameter. The colors indicate f .

Therefore the inferred γ depends on f as

$$\tan \gamma \propto f^{1/2} \frac{(Q^2 + U^2)^{1/4}}{V}. \quad (2)$$

For HMI's moderate resolution, f proves to be highly degenerate with B (Centeno et al. 2014). The HMI pipeline thus adopts $f \equiv 1$, which is appropriate when no additional information is available. However, the magnetic fields may be structured on scales smaller than the HMI resolution. For the polar magnetic patches, the distribution of f has a broad peak centered around 0.15 according to *Hinode* observations. If so, Equation (2) posits that HMI's unity f will incur a $|\tan \gamma|$ that is systematically too large, or, a \mathbf{B} vector too inclined toward the plane of sky.

We test this line of reasoning by re-inferring the HMI data with f as a free parameter (Griñón-Marín et al., in preparation). The values of f show a broad peak centered at about 0.25. The field vectors indeed become more radial, in particular for smaller f 's, even though the bias persists (Figure 1(c)). The degeneracy between f and B manifests in their correlation coefficients, most of which lie between -1 and -0.8 . Due to the degeneracy, the individual parameter uncertainties increase significantly.

Polar field observations from the Vector Stokes Magnetograph (VSM) instrument appear to have an opposite bias, i.e., the \mathbf{B} vectors systematically tilt toward the equator (Gosain et al. 2013). There is generally $|B_r| < |B_l| \mu^{-1}$ for VSM, and $|B_r| > |B_l| \mu^{-1}$ for HMI in the polar region. A VSM-HMI discrepancy of the field orientation also shows up in the plage region (Pevtsov et al. 2021). The differences are partially credited to the treatment of f , in line with our finding.

Previous work shows that the fine-scale fields cannot always be reliably inferred from low-resolution maps (Leka & Barnes 2012). The problem may benefit from high-resolution observations from the *Daniel K. Inouye Solar Telescope* (Rimmele et al. 2020) or out-of-ecliptic observations from the Polarimetric and Helioseismic Imager (Solanki et al. 2020) aboard the *Solar Orbiter*. They can provide more informative priors for f and γ , respectively. Synthetic data from numerical simulations will provide a useful benchmark for assessing the systematic biases (Plowman & Berger 2020).

We thank K. D. Leka for helpful discussions. X. Sun is supported by NASA HGiO award 80NSSC21K0736. The *SDO* data are courtesy of NASA and the HMI science team.

REFERENCES

Centeno, R., Schou, J., Hayashi, K., et al. 2014, *SoPh*, 289, 3531
 Gosain, S., Pevtsov, A. A., Rudenko, G. V., & Anfinogentov, S. A. 2013, *ApJ*, 772, 52
 Hoeksema, J. T., Liu, Y., Hayashi, K., et al. 2014, *SoPh*, 289, 3483
 Jefferies, J. T. & Mickey, D. L. 1991, *ApJ*, 372, 694
 Leka, K. D. & Barnes, G. 2012, *SoPh*, 277, 89
 Petrie, G. J. D. & Patrikeeva, I. 2009, *ApJ*, 699, 871
 Pevtsov, A. A., Liu, Y., Virtanen, I., et al. 2021, *SWSC*, 11, 14
 Plowman, J. E. & Berger, T. E. 2020, *SoPh*, 295, 144
 Rimmele, T. R., Warner, M., Keil, S. L., et al. 2020, *SoPh*, 295, 172
 Solanki, S. K., del Toro Iniesta, J. C., Woch, J., et al. 2020, *A&A*, 642, A11
 Svalgaard, L., Duvall, T. L., J., & Scherrer, P. H. 1978, *SoPh*, 58, 225
 Tsuneta, S., Ichimoto, K., Katsukawa, Y., et al. 2008, *ApJ*, 688, 1374
 Wang, Y. M. & Sheeley, N. R., J. 1992, *ApJ*, 392, 310